

## Article

# Flexural Strength of Concrete Beams Made of Recycled Aggregates: An Experimental and Soft Computing-Based Study

Ehsan Momeni <sup>1</sup>, Fereydoon Omidinasab <sup>1,\*</sup>, Ahmad Dalvand <sup>1</sup>, Vahid Goodarzimehr <sup>2</sup> and Abas Eskandari <sup>1</sup><sup>1</sup> Faculty of Engineering, Lorestan University, Khorramabad 68151-44316, Iran<sup>2</sup> Department of Civil Engineering, Shahid Bahonar University of Kerman, Kerman 76169-13439, Iran\* Correspondence: [omidinasab.f@lu.ac.ir](mailto:omidinasab.f@lu.ac.ir)

**Abstract:** The implementation of recycled concrete aggregates (RCAs) in the construction industry has been highlighted in the literature recently. This study aimed to propose an intelligent model for predicting the ultimate flexural strength of recycled reinforced concrete (RRC) beams. For this reason, a database comprising experimental tests on concrete beams was compiled from the literature. Additionally, two experimental tests were performed in the laboratory to enhance the aforementioned database. The flexural test results showed a 10% reduction in flexural strength when the RRC beam was tested instead of a conventional beam (constructed with natural aggregates). Nevertheless, an artificial neural network (ANN) improved by particle swarm optimization (PSO), as well as an imperialist competitive algorithm (ICA), were utilized for developing the predictive model. The inputs of the hybrid predictive models of flexural strength were the beam geometrical properties, reinforcement ratio, RCA percentage, compressive strength of concrete, and the yield strength of steel. The overall findings (e.g., correlation coefficient values of 0.997 and 0.994 for the testing data) showed the feasibility of the PSO-based ANN predictive model, as well as the ICA-based ANN predictive model in the flexural assessment of RRC beams. Furthermore, comparing the prediction performances of PSO-based ANN with ICA-based ANN and the conventional ANN showed that the PSO-based ANN model outperformed the predictive model built with the conventional ANN and the ICA-ANN.

**Keywords:** ANN; experimental test; flexural strength; ICA; PSO; recycled aggregate; soft computing



**Citation:** Momeni, E.; Omidinasab, F.; Dalvand, A.; Goodarzimehr, V.; Eskandari, A. Flexural Strength of Concrete Beams Made of Recycled Aggregates: An Experimental and Soft Computing-Based Study. *Sustainability* **2022**, *14*, 11769. <https://doi.org/10.3390/su141811769>

Academic Editor: Rajesh Kumar Jyothi

Received: 29 August 2022

Accepted: 16 September 2022

Published: 19 September 2022

**Publisher's Note:** MDPI stays neutral with regard to jurisdictional claims in published maps and institutional affiliations.



**Copyright:** © 2022 by the authors. Licensee MDPI, Basel, Switzerland. This article is an open access article distributed under the terms and conditions of the Creative Commons Attribution (CC BY) license (<https://creativecommons.org/licenses/by/4.0/>).

## 1. Introduction

The space limitation for construction in urban areas, waste disposal demolition, and the high renting costs of landfills is becoming a major problem. Many researchers underlined the beneficial effect of recycling concrete in minimizing the aforementioned problems to some extent [1]. The demand for new aggregates can be reduced considerably if recycled concrete aggregates (RCAs) are used. In other words, the utilization of RCA can lead to the preservation of resources, forested areas, and/or river beds. In fact, the beneficial effects of RCA utilization from the environmental point of view are considerable. Hossain et al. [2] mentioned that the implementation of coarse RCA in Hong Kong reduced the greenhouse gases footprints considerably. Many researchers investigated the feasibility of using RCA in the construction industry. Soutsos et al. [3] reported the workability of waste construction materials as aggregates for producing precast concrete products. Silva et al. [4] proposed a new method for using construction waste to produce concrete using a statistical analysis. In countries such as Japan, a considerable amount of concrete is recycled [5]. However, Kang et al. [6] mentioned that almost 14% of waste concrete is recycled.

Yehia et al. [7] conducted a comprehensive study on the effectiveness of using recycled aggregates for concrete production. Katerusha [8] reported that in 2018, the average recovery rate of construction in the European Union was about 90%. In Zurich, 90% of the utilized concrete between 2005–2018 comprised recycled aggregates. Although the use of RCA in a

non-structure application is permitted, many studies highlighted that the implementation of RCA in structural applications is also possible. Knaack and Kurama [9] investigated the flexural behavior of reinforced recycled concrete (RRC) beams. They reported that the effect of RCA on flexural strength is not considerable. Ignjatovic et al. [1] stated that there is no remarkable difference between the flexural failure load of RRC beams and conventional concrete beams. Arezoumandi et al. [10] performed full-scale tests and compared the flexural behavior of reinforced concrete beams made of concrete with natural aggregate and 100% RCA. According to their conclusion, in terms of strength, an RRC beam is comparable with conventional beams; however, in terms of deflections, conventional beams outperformed RRC beams (their observation showed 13% higher deflection in RRC beams). Almost the same conclusion was drawn by Sato et al. [5]. Choi et al. [11] also performed several full-scale tests to investigate the flexural performance of RRC beams. They also suggested that RRC beams can be implemented as load-carrying structures. Nevertheless, some researchers have pointed out that the amount of RCA also plays an important role in the ultimate flexural strength of beams. For example, Khatib [12] mentioned that coarse RCA up to 30% can be utilized as replacement aggregate without showing any strength reduction. Seara-Paz et al. [13] studied the flexural performance of RRC beams made with different RCA percentages (20%, 50%, and 100%). According to their results, when 100% RCA was utilized, a nearly 10% reduction in bending moments under the serviceability condition was observed. Adjukiewicz and Kliszczewicz [14] performed comparative tests on columns made of conventional concrete and recycled aggregate concrete. According to their study, a negligible difference in load-bearing capacities was observed. However, in terms of deformation, a word of caution is required in the deformation assessment of structural members that are made from RCA.

Bai and Sun [15] conducted an experimental study and compared the load-carrying capacities of conventional concrete beams with concrete beams constructed with 70% RCA. According to their findings, the bearing capacities of the two types of beams were in good agreement. They concluded that it is feasible to implement RCA in structural members that are made of concrete. Al-Zahraa et al. [16] reported that the flexural strengths of RRC beams are close to conventional concrete beams. Kang et al. [6] concluded that the flexural behavior of reinforced concrete beams was not remarkably affected when the replacement ratio of RCA was up to 30%. Overall, in terms of flexural performance, the aforementioned studies encourage the implementation of RCAs for concrete beams.

On the other hand, the feasibility of artificial intelligence (AI) in solving civil engineering problems has drawn considerable attention in recent past years [17–26]. For example, Ateris et al. [27] suggested the implementation of soft computing techniques for predicting the compressive strength of concrete. Le et al. [28] recommended the utilization of machine learning techniques for assessing the load-carrying capacity of concrete-fill steel tube columns. Naderpour and Mirrashid [29] assessed the shear strength of reinforced concrete beams using an adaptive neuro-fuzzy inference system (ANFIS). They used 194 sets of data for their model development. The input parameters of their proposed model included the geometrical properties of beams, as well as the strength properties of the concrete and reinforced bars.

Lu et al. [30] proposed tree-based predictive models for assessing the punching shear capacity of concrete flat slabs that were reinforced with steel fibers. They implemented 140 sets of data to train their models. They used six input parameters, including the reinforcement ratio and compressive strength of concrete. According to their results, a random tree coupled with their proposed novel feature selection technique could provide a feasible tool for predicting the punching shear capacity of concrete slabs.

In another study, Asteris et al. [31] proposed an ANN-based predictive model of the compressive strength of a masonry prism. They compiled 232 sets of data from the literature to develop their model. Overall, their findings showed that ANN is a powerful and reliable tool for masonry compressive strength prediction.

Kamanli et al. [32] proposed an ANN-based predictive model for assessing the flexural behavior of reinforced concrete beams. The coefficient of determination ( $R^2$ ) equal to 0.96 for testing data suggested that their recommended predictive model was good enough. It is worth mentioning that the input parameters of their model comprised the reinforcement ratio, compressive strength of concrete, cement dosage, elastic modulus of concrete, yielding stress of steel, ultimate strength of steel, and load. The deflection was set as the model output in their ANN-based predictive model. They used 82 experimental sets of data to train their intelligent model. Perera et al. [33] utilized ANN to predict the ultimate shear strength of reinforced concrete beams.

Kaczmarek and Szymanska [34] also highlighted the workability of ANN in predicting the deflection of reinforced concrete beams. They used 293 sets of data for their model development. The input parameters of their model included Young's modulus of concrete, Young's modulus of steel, the surface area of tension reinforcement, and the bending moment. The geometry of the beam was omitted from their study. Bai et al. [35] promoted implementations of ANN, support vector machine (SVM), and adaptive neuro-fuzzy inference system (ANFIS) for assessing the deflection of reinforced concrete beams. They used 120 sets of data for their model development. The input parameters of their proposed models were the tensile strength, beam length, compressive strength, shear span–depth ratio, applied load, percentage of stirrups, and percentage of reinforcement.

Suguna et al. [36] proposed an ANN-based predictive model for the flexural assessment of high-strength concrete. They used fiber-reinforced polymer (FRP) laminates for concrete strengthening. The input parameters of their developed model were the beam geometrical properties (length, depth, width), reinforcement ratio, concrete compressive strength, tensile strength, and elasticity modulus of FRP laminates. According to their study, different output parameters, including the service load and ultimate load, were used. Overall, their study showed that ANN is a useful technique for assessing the aforementioned problem. Another ANN-based study was performed by Metwally [37]. The output of his proposed model was the ultimate load. He used 14 input parameters to construct his intelligent model. Shanmugavelu et al. [38] also highlighted the workability of ANN in assessing the performance characteristics of reinforced concrete beams strengthened with glass FRP laminates.

Saadoon and Malik [39] developed an ANN-based model for predicting the ultimate load of a concrete beam that was strengthened with FRP bars. They used 199 sets of data collected from the literature for their model construction. The proposed model consisted of eight input parameters. The input parameters of their model consisted of the cross-sectional width and depth of the beams, cross-sectional area, elasticity modulus, tensile strength of FRP bars, compressive strength of concrete, effective span length, and shear–span ratio. Al-Jurmma [40] also showed that ANN is a feasible tool for predicting the ultimate load capacity of reinforced concrete beams. The database of their ANN-based predictive model was constructed using finite-element-based numerical analyses.

Erdem [41] suggested an ANN-based predictive model of moment capacity for reinforced concrete slabs. They used 294 sets of data for their model construction. Cai et al. [42] suggested an ANN-based predictive model that was enhanced with a genetic algorithm to assess the postfire flexural capacity of reinforced concrete beams. They used 480 sets of data, which were produced with the aid of finite element analyses. The input parameters of their proposed model comprised the height and width of the beams, cross-sectional area and tensile strength of reinforcement, compressive strength and cover of concrete, and fire time. The coefficient of determination value of 0.99 showed that a GA-based ANN was a quick and feasible tool for flexural capacity prediction.

This study was aimed toward proposing intelligent models that were optimized using particle swarm optimization (PSO) and imperialist competitive algorithm (ICA). The PSO-based ANN and ICA-based ANN models were developed for predicting the flexural strength of concrete beams that were made from recycled aggregate. Although the implementation of conventional ANNs for concrete beams is not new, it is well established

that the conventional ANNs suffer from some disadvantages, such as getting trapped in local minima and a slow rate of learning. Optimization algorithms, such as PSO and ICA, can enhance the performance of ANNs and overcome their shortcomings [26]. The main difference between the presented study and previous works is the point that in this study, ANNs were coupled with ICA and PSO for the flexural assessment of RRC beams. Apart from the artificial intelligence components, this paper presents the flexural performance of two experimental tests. The results of the two loading tests on concrete beams were added to the compiled sets of data that were obtained from literature and used for the predictive models' construction. Presenting the results of experimental tests is always of interest as these results can be utilized for enriching the related databases for further soft computing works. Nevertheless, after reviewing the related works in this section, in Section 2 of the presented paper, the utilized artificial intelligence methods are discussed. Section 3 deals with the implemented experimental program. In Section 4, the PSO-based ANN and the ICA-based ANN modeling procedures are discussed. Section 5 deals with the main results and discussion, and finally, the last section deals with the summary of the paper and concluding remarks.

## 2. Methods

In this section, the proposed methodology for predicting the flexural strength of concrete beams is discussed. At first, some explanations about ANN, PSO, and ICA are provided, and finally, the hybridization of the mentioned methods is proposed.

### 2.1. Artificial Neural Network

The use of artificial neural networks (ANNs) has become so pervasive among researchers. Artificial neural networks can be used for any system that requires analysis, decision-making, estimation, forecasting, design, and construction. In all these models, a mathematical structure is considered. This general structure is tuned and optimized using a training algorithm so that it can behave accurately. In civil engineering, ANNs are mostly considered good function approximation tools, especially for nonlinear problems. One of the most basic neural models available is the multi-layer perceptron (MLP), which was described by Dreyfus [43]. In this type of neural network, which is also called a feed-forward neural network, the behavior of the human brain is mimicked. Feed-forward ANNs are mainly made of three layers: the input layer, hidden layer, and output layer. Each layer comprises one or more neurons (also called nodes). The main engine of the ANNs is the hidden layer, where the hidden nodes receive information from the input layer (the influential parameters on the model output). It is worth mentioning that the information is transferred between layers through connection weights, as well as threshold values, which are called bias values. The net input of each hidden node is the summation of input weights plus the bias value of the specific hidden node. The outputs of the hidden nodes are determined after applying transfer functions (often sigmoid functions) on the net inputs of the hidden nodes. This process continues until a reasonable output is achieved. It is worth mentioning that the connection weights have to be adjusted using training algorithms until the point that the error between the network outputs and target values is minimized. The aforementioned error is often assessed using the mean square error (MSE) of the system or root-mean-square error (RMSE) of the system.

### 2.2. Particle Swarm Optimization Algorithm

The PSO algorithm is one of the most significant intelligent optimization algorithms, which is based on swarm intelligence. The PSO algorithm was first developed by Kennedy and Eberhart [44]. The particle swarm optimization algorithm has a memory so that the knowledge of possible solutions is reserved for all particles. Each member of the swarm changes their position according to personal experiences and the experiences of the whole society. The social sharing of information between members of society has some advantages, and this hypothesis is the basis of the particle swarm optimization algorithm.

In the PSO method, after the initialization of the population, the particles usually converge in successive iterations of the local search process in a feasible space. PSO works with two simple equations. The position and the velocity of each particle are defined through Equations (1) and (2):

$$X_i^{k+1} = X_i^k + V_i^{k+1} \quad (1)$$

$$V_i^{k+1} = c_1 r_1 (P_i^k - X_i^k) + c_2 r_2 (P_g^k - X_i^k) \quad (2)$$

where  $V_i^{k+1}$  and  $X_i^k$  are the  $i$ th particle's velocity and position at  $k$  and  $k + 1$  iterations, respectively;  $c_1$  and  $c_2$  are two acceleration constants;  $P_i^k$  is the best position of the  $i$ th particle up to iteration  $k$ ; and  $P_g^k$  is the best position among all particles in the swarm up to iteration  $k$ . In Figure 1, the velocity updating process is shown.

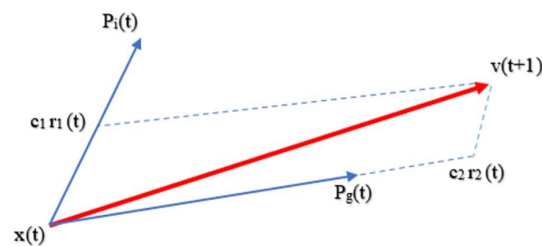


**Figure 1.** The updating scheme of the velocity.

### 2.3. Imperialist-Competitive-Algorithm-Based ANN

In order to study the effect of different optimization algorithms on the ANN performance and to enrich the soft computing part of the study, the imperialist competitive algorithm (ICA) was also utilized to improve the ANN performance. Details on the ICA are beyond the scope of this study and can be found elsewhere [45,46]. Nevertheless, the ICA as a global search algorithm starts with generating a user-defined number of so-called countries that play the role of particles in PSO. Like PSO, each country (particle) can be a potential solution to the problem. However, unlike PSO, in the ICA, the countries are categorized into imperialists and colonies. In fact, countries are sorted based on their fitness. The fitness function (sometimes it is called the cost function) in most engineering problems is the computed error between the predicted and measured values (often the mean square error (MSE)). Nevertheless, the proper number of imperialists, which are the fittest countries (i.e., countries with the lowest MSE values) can be determined after a trial-and-error procedure. The remaining countries are so-called colonies.

A certain number of colonies are assigned to each imperialist (empire) based on the empire's power (normalized cost of each empire). Consequently, more powerful empires have more colonies. For a better understanding, the most powerful empire is the country with the lowest MSE value. In fact, designers set an initial number of countries and imperialists; subsequently, they investigate the model performance. Like PSO, an iteration process (in the ICA, it is called a decade) is required for optimization. The proper number of decades can also be obtained using a trial-and-error procedure.

In essence, the ICA works with its three operators: assimilation, revolution, and competition. Colonies will be attracted to the empires using assimilation. Revolutions can suddenly alter the positions of the countries. It is worth mentioning that during assimilation and revolution, a colony may reach a state that is better than its empire state. In competition, imperialists try to obtain more colonies, and all empires attempt to take possession of the colonies of other imperialists. All the imperialists have the chance to take control of at least one colony of the weakest empire (based on the imperialists' power). Hence, during competition, the weak empires start to collapse, and on the other hand, the more powerful imperialists gain more power and expand their empires. This process often continues until a designer-defined termination criterion such as the maximum number of decades is met. At last, the most powerful empire (the country with the lowest MSE value) represents the solution to the problem of interest.

#### 2.4. Hybrid ANNs (PSO-Based ANN and ICA-Based ANN)

The artificial neural network is often utilized for prediction and cannot perform search operations. In fact, the process of training in the ANN requires weight optimization. In supervised ANNs, the network receives a training algorithm and calculates the output using the weights in the randomly assigned network. However, many researchers highlighted that the slow rate of learning is one of the major drawbacks of ANNs (e.g., Momeni et al. [47]). The neural network can help to some extent but does not guarantee that the optimal answer is fully shown and converged toward. In fact, it is well established that getting trapped in local minima is another drawback of ANNs [48].

The idea of improving the ANN performance with the aid of global search algorithms, such as PSO, was proposed in previous studies for other applications, mainly due to the point that the neural network results are not necessarily the global optimal solutions [49]. In fact, PSO can be implemented for the weight optimization of ANNs. The PSO algorithm's initial population comprises the possible ANN weights (each particle contains the whole ANN weights). The PSO algorithm, which has a high power of global exploration, can easily obtain the optimal global answer by sharing information between particles. In order to better understand the hybrid process of PSO-based ANN, the optimization process is shown in the following flowchart (see Figure 2). It is worth mentioning that the hybrid process of an ICA-based ANN is similar to the PSO-based ANN, except that in an ICA-based ANN, the ICA algorithm is implemented to optimize the ANN weights.

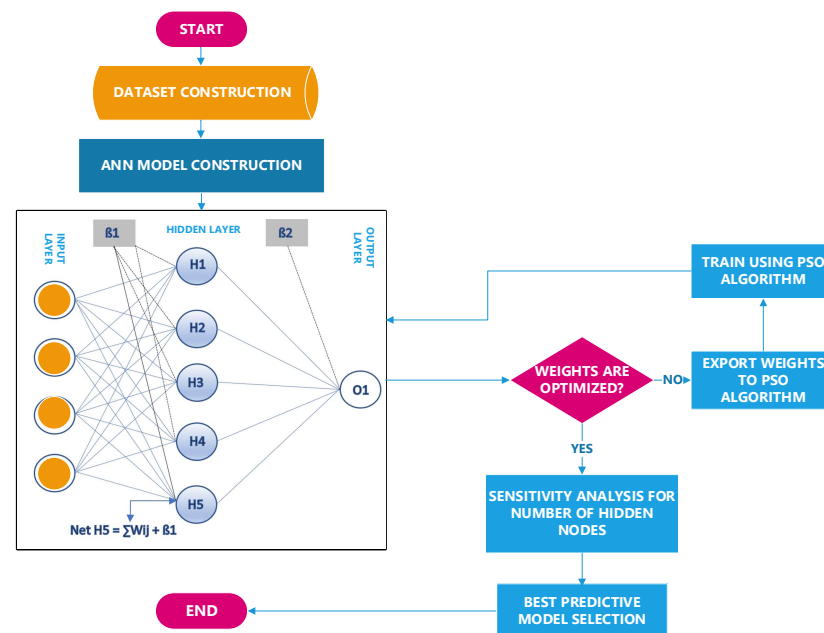


**Figure 2.** Flowchart of the hybrid PSO-based ANN model.

### 3. Experimental-Based Dataset

A comprehensive database plays a crucial role in designing AI-based predictive models. It is well established that the size of database can enhance the efficiency of the predictive models. Nevertheless, in civil engineering problems where performing numerous experiments is a difficult task to be accomplished, compiling different sets of data from literature is common, especially when the scope of a study is on highlighting the feasibility of soft computing techniques. Therefore, this study mostly used the previously published data in the literature.

However, in this study, to enrich the quality of the work, apart from compiled data from literature [1,5,9–11,13–16,50], the results of two experimental tests performed in the Structural Laboratory of Lorestan University were added to the aforementioned database. The experimental procedure for the tests is highlighted in the next section.

Overall, 107 sets of data were used in this study. It is worth mentioning that in the context of AI-based predictive models, setting several input parameters, as well as an output parameter(s), is essential. Any parameter can be set as an input for the predictive model if there is a meaningful relationship between the input and output parameters [51]. In the case of necessity, a sensitivity analysis can be implemented to reduce the number of influential parameters.

The input parameters used in this study comprised the compressive strength of concrete, longitudinal reinforcement ratio, the width of the beam, effective depth of the section, amount of RCA in terms of the percentage, span's-length-to-effective-depth ratio, yield strength of steel, and ratio of the distance of the applied load from the beam edge to the effective depth of the beam. The output parameter was the flexural strength of the beam. Table 1 shows the summary of the implemented dataset in this study.

**Table 1.** Summary of the data used in this study.

Symbol *	Type	Unit	Minimum	Maximum	Average
RCA	Input	%	0	100	50
B	Input	mm	100	400	185
d	Input	mm	160	525	245
a/d	Input	-	1.92	5.14	3.57
L/d	Input	-	4.81	17.5	11.16
$\rho$	Input	-	0.28	2.54	1.06
$f_c$	Input	MPa	26.8	105.3	44
$F_y$	Input	MPa	318	640	460
Mu	Output	kN·m	8	879	75

\* RCA: recycled concrete aggregate, B: width of the beam, d: effective depth to the flexural reinforcement, a/d: ratio of the distance of the applied load from the beam edge to the effective depth of the beam, L/d: ratio of the beam length to the effective depth,  $\rho$ : longitudinal reinforcement ratio,  $f_c$ : compressive strength of concrete,  $F_y$ : yield strength of steel.

#### *Experimental Procedure of the Performed Tests*

In order to investigate the flexural performances of the reinforced beams, first, the raw materials were prepared (cement, natural and recycled aggregates). It should be mentioned that in this study, ordinary Portland cement (ASTM type II) was used according to ASTM C150 [52]. The chemical properties of the utilized cement are shown in Table 2. The natural aggregates with a maximum size of 10 mm were obtained from the Khorramabad River. On the other hand, the preparation of the recycled concrete aggregate had several stages. The first stage dealt with crushing the old concrete specimens by using a crusher machine. Subsequently, these materials were washed and granulated into coarse and fine aggregate. In this research, to achieve a high-quality recycled aggregate (RA), four hundred cubic old concrete specimens with dimensions of  $150 \times 150 \times 150$  mm were chosen. These cubic specimens (see Figure 3) were collected from Structure Laboratory at Lorestan University and were crushed in accordance with ASTM D8038 [53] and ACI 555 [54]. In this study, the coarse RA had a maximum size of 9 mm according to ASTM C125 [55], and it had a fractured percentage of more than 87%, conforming to ASTM D5821 [56].

**Table 2.** Chemical properties of the utilized cement.

Chemical Composition	L.O.I	SiO <sub>2</sub>	Al <sub>2</sub> O <sub>3</sub>	Fe <sub>2</sub> O <sub>3</sub>	CaO	SO <sub>3</sub>	MgO
%	1.05	21.5	5.1	4.4	63.2	2.1	1.75



**Figure 3.** The utilized cubic specimens.

In the next stage, to investigate the workability of the RCA, two 1500 mm reinforced concrete (RC) beams with a width of 200 mm and a height of 300 mm were constructed and tested. These specimens were subjected to a concentrated load in the middle of their span, and the loading process was continued until the failure occurred. The geometrical properties of these concrete beams are presented in Figure 4. As can be seen from Figure 4, three T14 steel bars were used as a longitudinal tension bar, two T10 steel bars were utilized as a compression bar, and ten T10 steel bars were used as a stirrup for each specimen. The tensile stress test was performed on the steel bars in accordance with ASTM C370 [57].

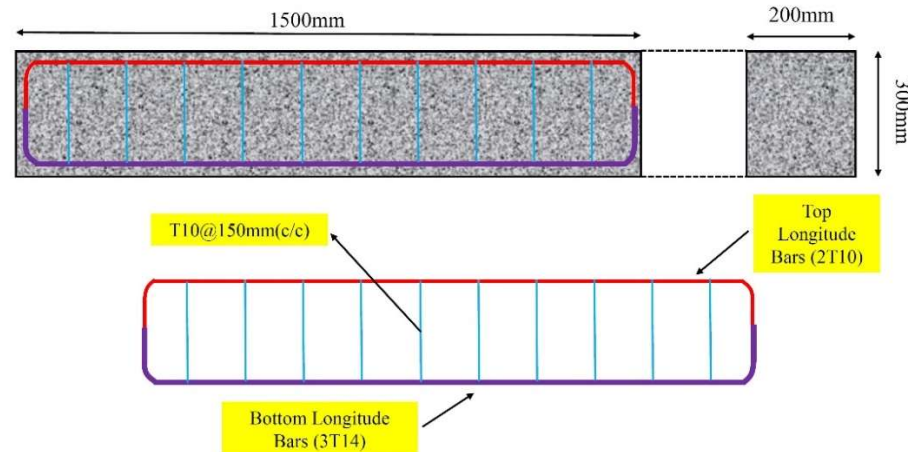


**Figure 4.** Reinforcement detail of the constructed beams.

The longitudinal bars with diameters of 14 and 10 mm had yielding stresses of 293 and 369 MPa, respectively. Furthermore, these bars had failure stress of 520 and 562 MPa. Based on the tensile test results, the yielding and failure stresses of the used stirrups were 281 and 508 MPa, respectively. For the purpose of brevity, the aforementioned results are not discussed here. In this research, to investigate the effects of RAs on the flexural behavior of reinforced concrete beams, the two abovementioned beams were tested under pure bending. The specimens had the same rebars and dimensions, but in terms of the aggregate, they were made of natural aggregate and RAs. It is worth mentioning that the aggregates used in both beams had the same gradation. Figure 5 shows the distribution curves of the recycled aggregates.

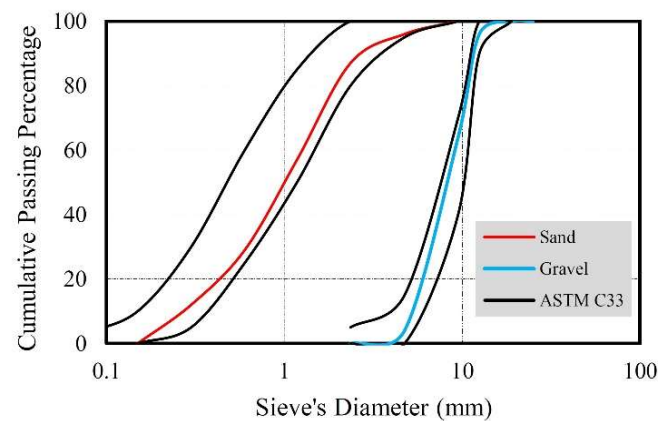


**Figure 5.** The gradation curve of the implemented (recycled) aggregates.

For the concrete construction, first, fine and coarse aggregates were added to the mixer and after three minutes, the cement and water were added to the aggregates and mixed for two more minutes. After making the concrete, it was poured into the beam mold, and after 28 days of curing the specimens, they were tested. As shown schematically in Figure 6, the beams were subjected to a net bending test in the middle of the span. Three LVDTs were used to measure the displacement of the specimens. Moreover, using a load cell with a capacity of 500 kN, the applied force was measured. The load applied to the beams was in the form of displacement control. The loading process continued until the specimens collapsed. Figure 7 shows the mid-span displacement versus the applied force. The maximum load capacity of the RRC beam was approximately 10% less than the reference beam (RC beam) (including natural aggregate). Furthermore, this behavior was acceptable in accordance with the RA features. As we know, flexural behavior in concrete beams depends on the compressive and tension zones of specimens. According to the results, having a rough surface had a profound effect on flexural behavior. Additionally, the natural aggregates had rougher surfaces in comparison with the RAs; thus, this feature had a large effect on the aggregate–cement bond strength. The concrete ultimate strain rose with an increase in the interlock between the cement paste and aggregate’s surface. In fact, increasing the adhesion of cement affected the ultimate flexural strength of the beam specimens.

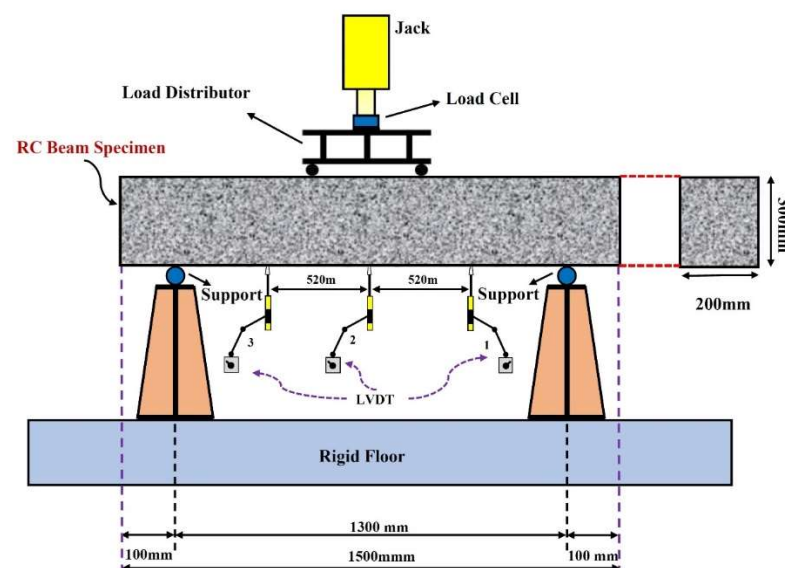


**Figure 6.** Schematic figure of the test set-up.

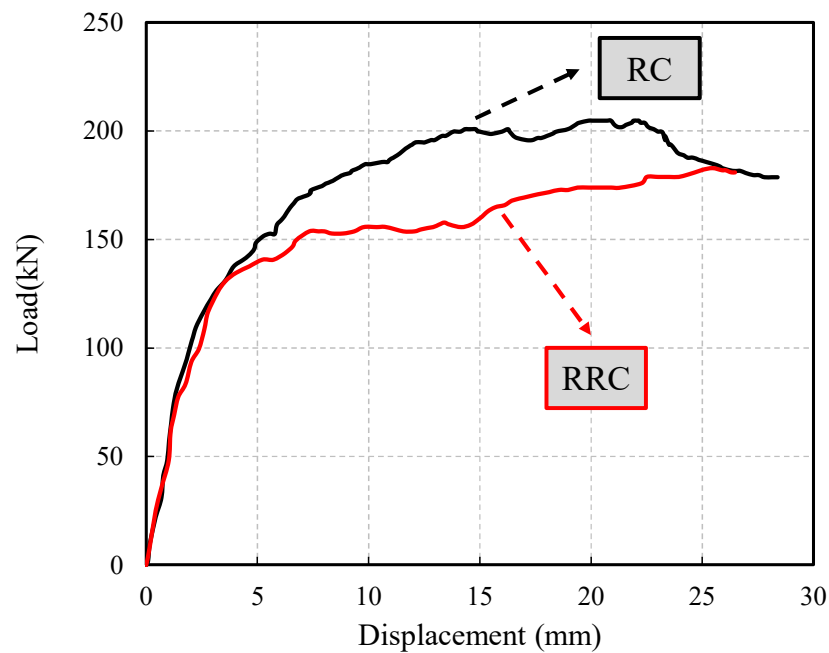


**Figure 7.** Load–displacement curve of the performed flexural tests.

Based on the experimental results, the initial slopes of the load–displacement curve for the two beams were approximately similar. When the applied load reached 40% of the ultimate load capacity, the linear behavior changed to nonlinear behavior. The flexural behaviors of the beams showed that with an increase in the load up to 40% of its ultimate capacity, the longitudinal rebars could reach their yielding strength. Moreover, the yielding process was accompanied by crack propagation on the beam’s surface.

Concerning the results, tri-linear behavior could be assumed for beam specimens, and this behavior was classified into three steps. The occurrence of the first cracks in the mid-span was identified as the first stage. The yielding and collapse processes were recognized as the second and third stages in this study, respectively. The failure mode of the RRC beam was different compared with another specimen. The compressive zone failure dimension, crack width, shear-bending cracks, and crushing nature of the concrete were seen as the main differences. In this regard, Figure 8 shows the crack propagation of the RRC beam and the conventional reinforced concrete (RC) beam after failure.

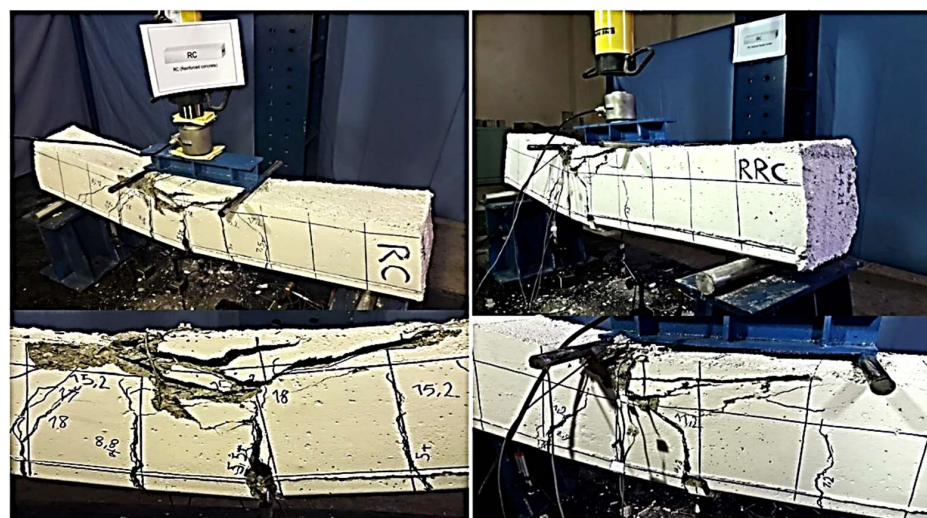


**Figure 8.** Post-failure behavior and crack propagation of specimens: RC beam (left side) and RRC beam (right side).

Overall, a comparison of the load capacity curves for the two beams showed that the corresponding displacement of the failure point for the RRC beam was almost 10% less than that of the RC beam. It is worth mentioning that for the purpose of brevity and owing to the nature of this work, the experimental results are not discussed in detail.

#### 4. Soft Computing Modeling Procedure

##### 4.1. PSO-Based ANN Modeling Procedure

As mentioned earlier, in PSO-based ANN modeling, the ANN weights are imported into the PSO algorithm, and after optimization, the optimized weights are exported into ANN for prediction purposes. Hence, before the ANN structure configuration, sensitivity analyses should be performed on the parameters of the PSO algorithm. The first usual sensitivity analysis is often implemented to determine the optimal number of iterations. For this reason, the number of iterations was set to 100 for a default PSO-based ANN model with nine hidden nodes. It is worth mentioning that the PSO coefficients, i.e.,  $C_1$  and  $C_2$ , were set as 2 for the primary sensitivity analysis. The primary number of particles was set to 200. Figure 9 shows the influence of the number of iterations on the performance of the PSO-based ANN predictive model. This figure suggests that after 40 iterations, there was a negligible change in MSE; hence, the number of iterations used during the sensitivity analyses was set to 40.

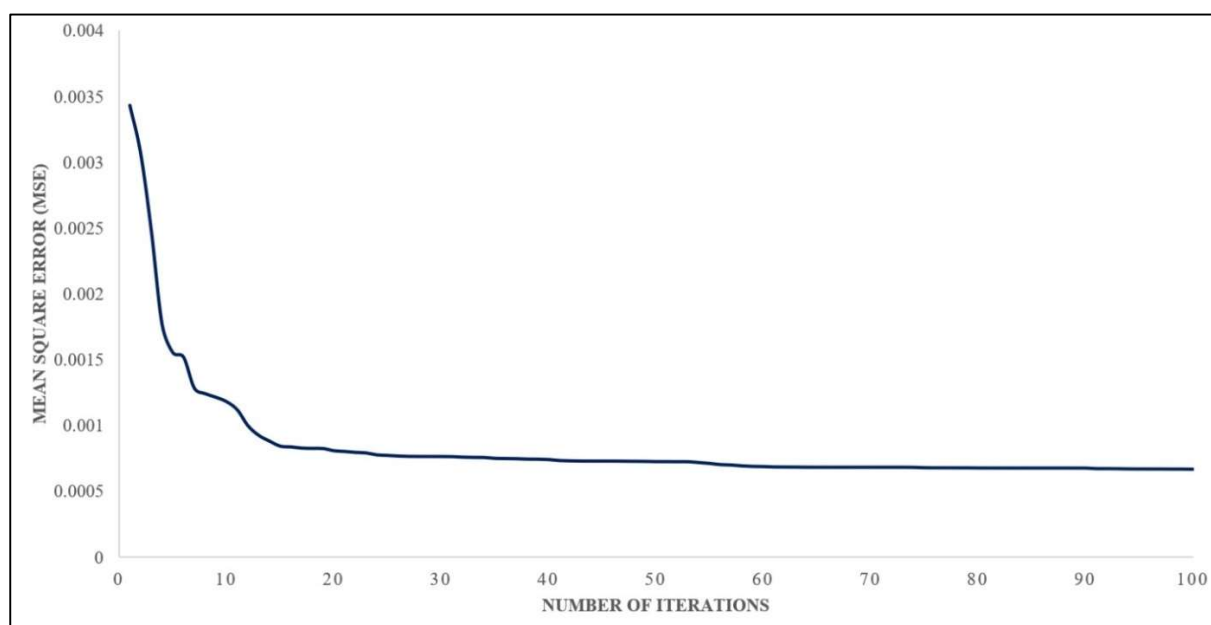


**Figure 9.** The effect of the number of iterations on the PSO-based ANN predictive model.

After determining the optimal number of iterations, the optimal number of particles, as well as the proper values for  $C_1$  and  $C_2$ , should be identified. For this reason, the effect of the number of particles on the model performance was investigated. For this reason, several models with 100, 150, 200, 300, 400, and 500 particles were run and it was found that the number of particles had no remarkable effect on the model performance, which was in good agreement with the authors' previous works [47]. On the other hand, to investigate the importance of PSO coefficients, the effect of considering different values for  $C_1$  and  $C_2$  was taken into consideration. For the purpose of brevity, details on the sensitivity results are not presented here; however, it was found that setting the values of  $C_1$  and  $C_2$  equal to 2 can lead to an acceptable prediction performance; hence, the aforementioned values were set to 2, as suggested in the literature [48]. It is worth mentioning that when the results of the sensitivity analyses were close to each other, the performance of the testing data was considered. It should be underlined that in all the analyses, 80% of the data

were considered for training the predictive model and the remaining data were used to test the developed model. After identifying the proper values for PSO parameters, the best ANN structure should be defined. In other words, the optimal number of hidden nodes should be identified. Researchers often implement two approaches to determine the optimal number of hidden nodes: using suggested equations and/or a trial-and-error procedure. In this study, a trial-and-error procedure was implemented to determine the optimal number of hidden nodes. The effects of 7, 8, 9, 10, 11, and 12 hidden nodes on the model performance was investigated. It was found that when nine hidden nodes were used in the PSO-based ANN predictive model, the model performed the best. For the purpose of brevity, only the results of the PSO-based ANN predictive models with 8 and 9 nodes are presented in Figures 10 and 11, respectively. It is worth mentioning that to reduce the likelihood of accidental results, each model was run five times. Nevertheless, as suggested in Figure 11, the second predictive model coefficient correlation of 0.997 and MSE of 0.08% for testing data outperformed other models. The overall results of different runs with nine hidden nodes showed that the PSO-based ANN predictive model worked well enough, as shown in Figures 10 and 11. The nine-node predictive model outperformed the eight-node predictive model, although the results of the latter were also reliable to some extent. The best results are illustrated in a better way in the Main Results and Discussion section.

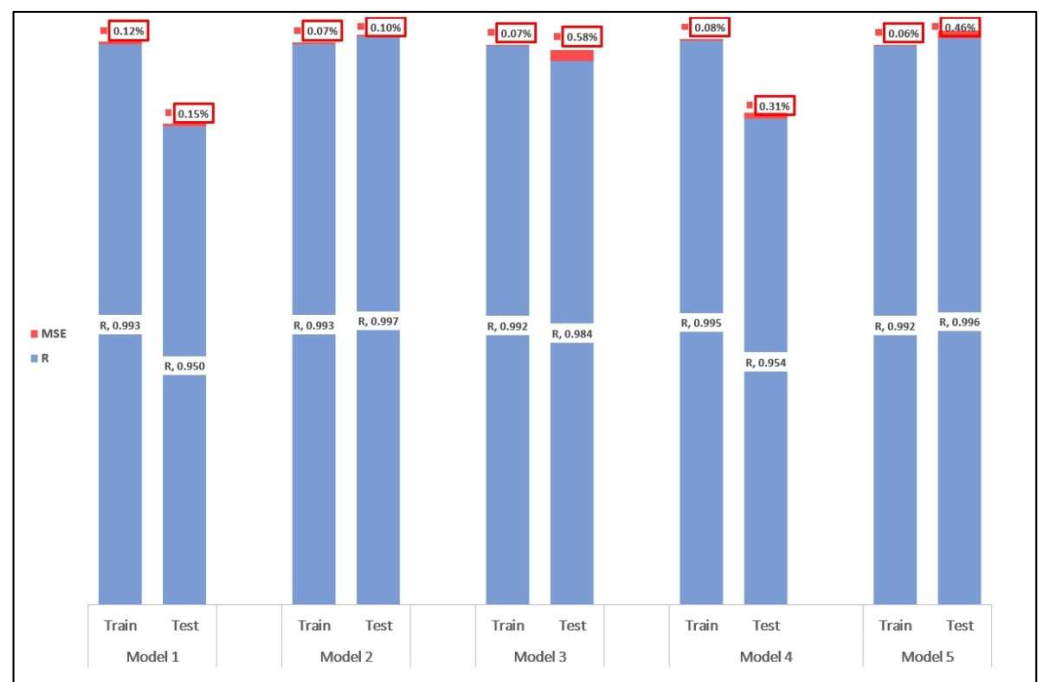


**Figure 10.** Prediction performances of the 8-node PSO-based ANN predictive model.

#### 4.2. ICA-Based ANN Modeling Procedure

The first step in developing the ICA-based ANN model dealt with identifying the optimal number of decades. For this reason, a default model had to be considered. The considered default model comprised 200 countries with nine hidden nodes in one hidden layer. A total of 10% of countries were set to be imperialists. The initial number of decades was set to be 100. Similar to the PSO-based ANN model, 80% of the data was assigned to train the model and the remaining data were used to test the prediction performance of the model. Figure 12 shows the variation of MSE values versus the number of decades. This figure suggests that after 36 decades, the change in MSE was negligible; hence, the optimal number of decades was set to 36 for further analysis. Identifying the optimal number of countries and imperialists was the next performed sensitivity analysis for developing the ICA-based ANN model. For this reason, the number of countries varied from 125 to 400, as

shown in Table 3. This table also showed the number of imperialists' variations. Similar to the previous section, the utilized performance indices were the R and MSE values. When the prediction performances of different models were close to each other, the prediction performance of the testing data was preferred.

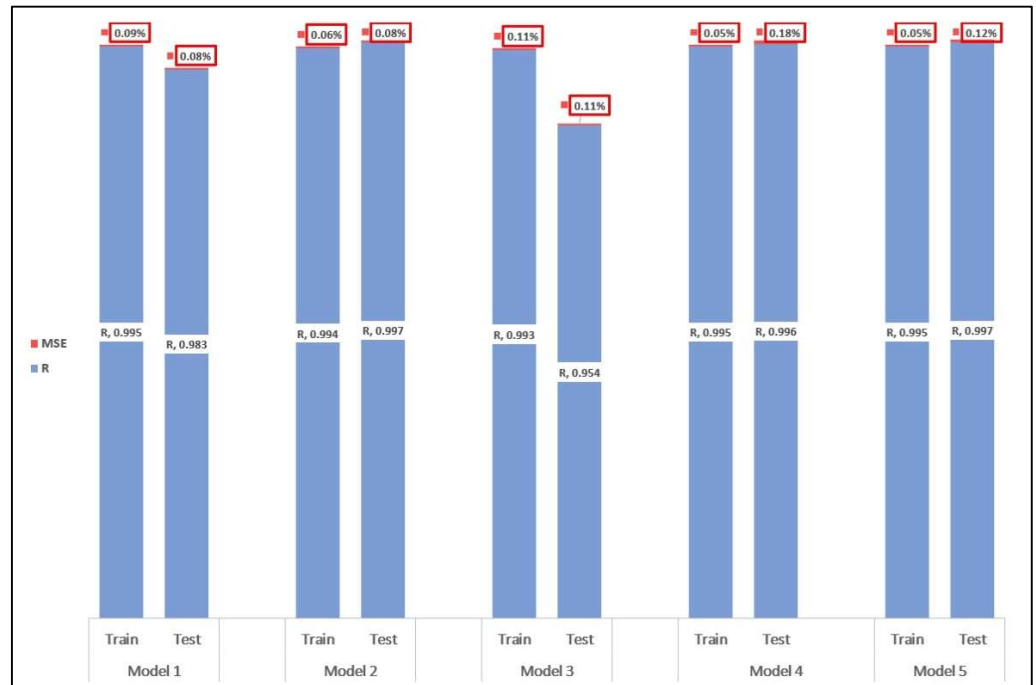


Figure 11. Prediction performances of the 9-node PSO-based ANN predictive model.

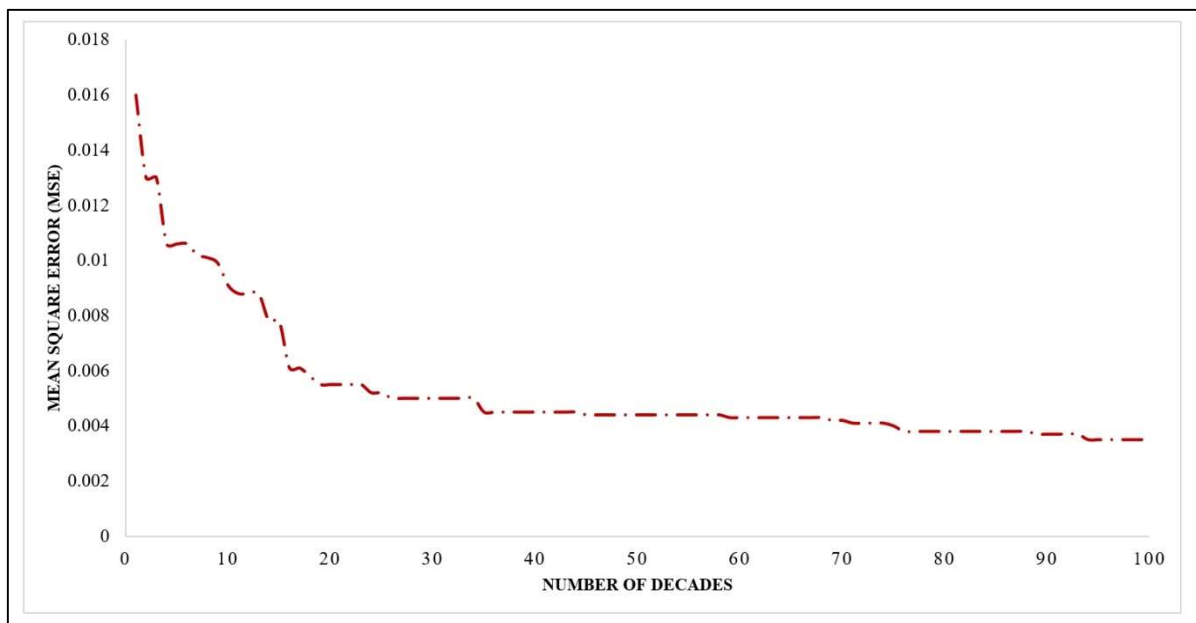


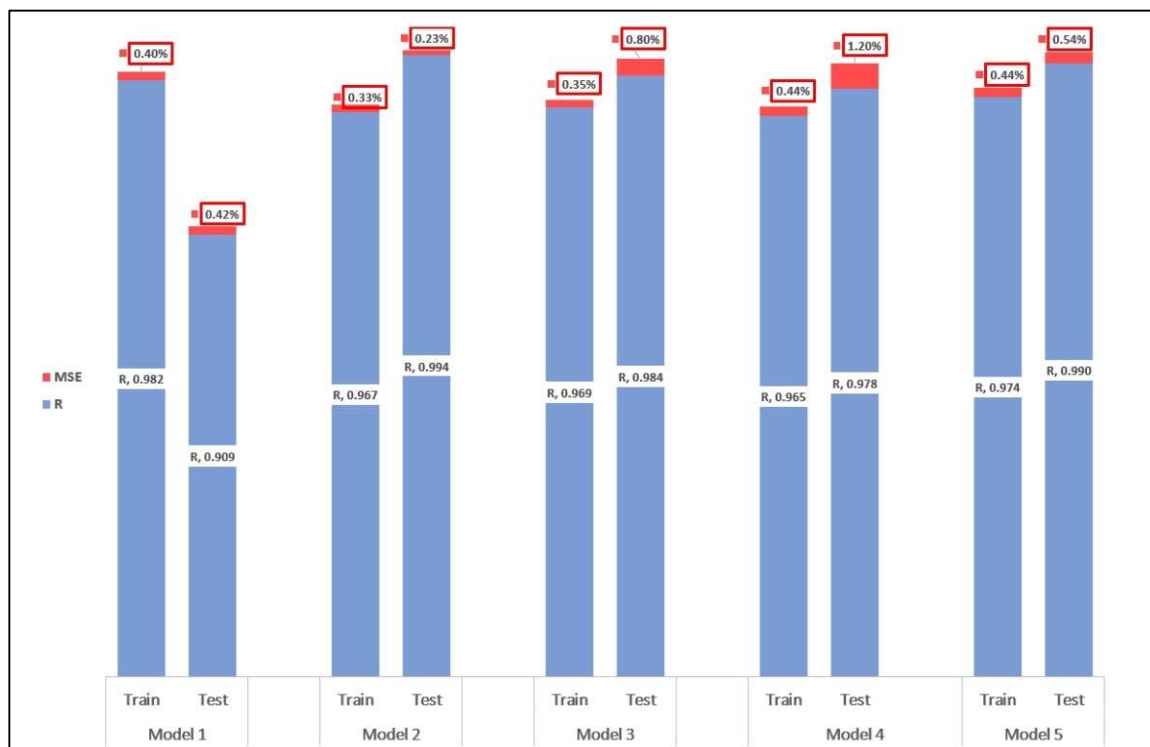
Figure 12. The effect of the number of decades on the ICA-based ANN predictive model.

Table 3 also shows the results of the aforementioned sensitivity analysis. The results presented in this table suggested that the best prediction performance of the ICA-based ANN predictive model was good enough when the numbers of countries and imperialists were 200 and 20, respectively. Hence, during the model development process, these default values were considered as the optimal number of countries and imperialists, respectively.

**Table 3.** The effect of ICA parameters on the prediction performances of the models.

Model No.	Parameter		Training Data		Testing Data	
	No. of Countries	No. of Imperialists	R	MSE	R	MSE
1	125	10	0.954	0.049	0.875	0.049
2	125	5	0.979	0.0040	0.843	0.0062
3	200	20	0.969	0.0035	0.984	0.008
4	200	10	0.976	0.0024	0.901	0.0317
5	200	15	0.967	0.0043	0.968	0.0115
6	250	15	0.968	0.0034	0.965	0.0201
7	300	30	0.976	0.0043	0.857	0.025
8	300	15	0.972	0.0033	0.974	0.0082
9	300	20	0.982	0.0036	0.904	0.0038
10	400	40	0.979	0.0045	0.856	0.0052
11	400	30	0.939	0.0060	0.982	0.0075
12	400	20	0.981	0.0039	0.905	0.0114

At last, to obtain a better comparison, the ICA-based ANN model with nine hidden nodes in one hidden layer was iterated five times (similar to the PSO-based ANN model to reduce the likelihood of accidental results). The prediction performances of the nine-node ICA-based ANN predictive models are shown in Figure 13. As shown in this figure, the R and MSE values (0.994 and 0.023) of the testing data suggested that the second model performed the best.

**Figure 13.** Prediction performances of the 9-node ICA-based ANN predictive model.

## 5. Main Results and Discussion

Figure 14 shows the prediction performance of the PSO-based ANN predictive model of the flexural strength of the RRC beams. The correlation coefficient of 0.994 for the training data showed that the predictive model worked well enough. On the other hand, Figure 15 displays the predicted flexural strengths of the RRC beams versus the measured values for the testing dataset. As shown in this figure, the correlation coefficient of 0.997 suggested that the PSO-based ANN model was a capable and feasible tool for assessing the flexural behavior of RRC beams. It is worth mentioning that MSE values for the training and testing data were 0.06% and 0.08%, respectively.

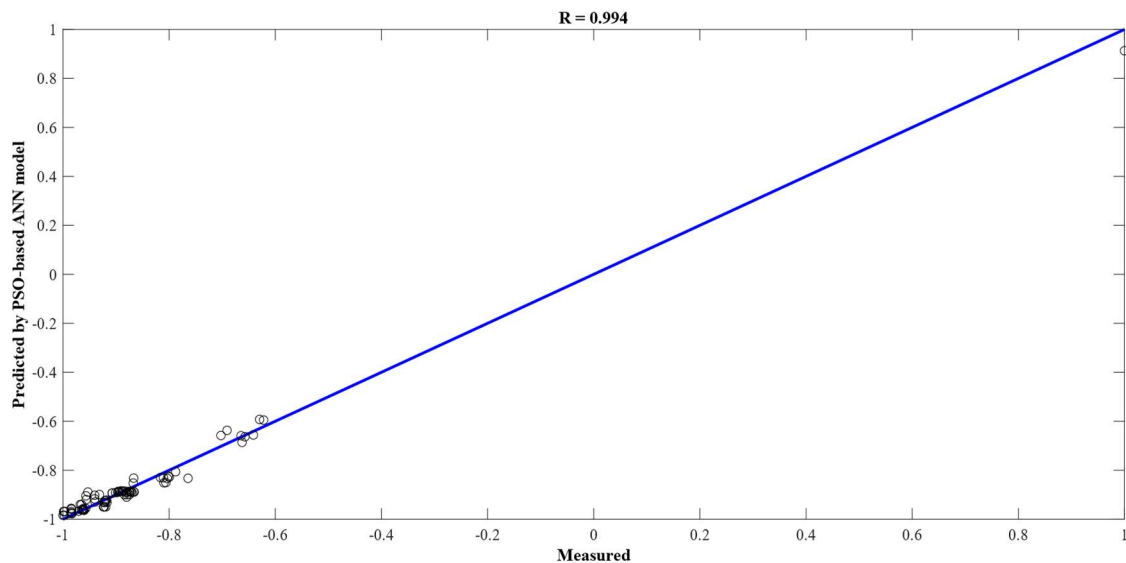


**Figure 14.** Prediction performance of the proposed PSO-based ANN model (training data).

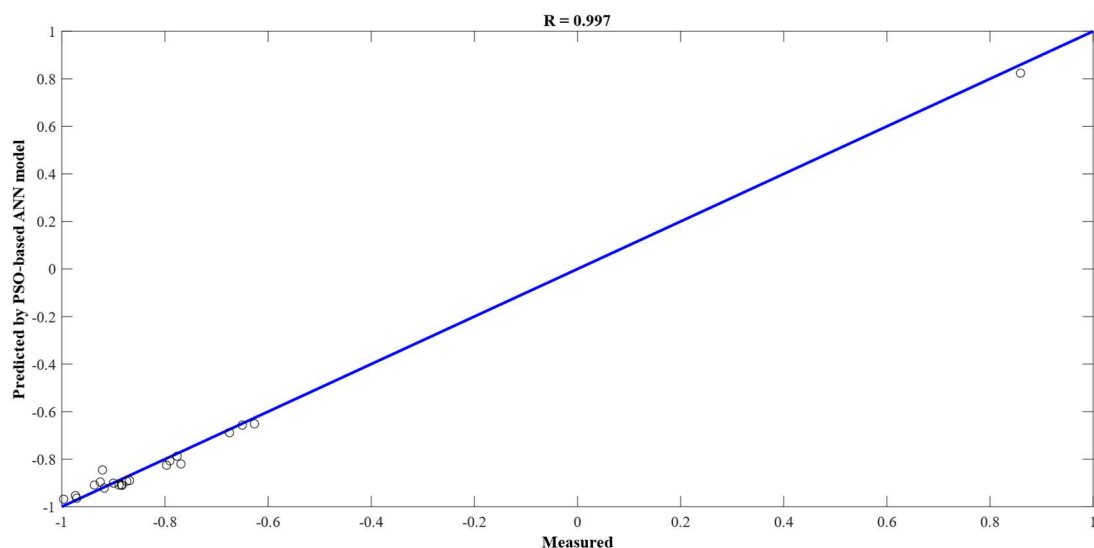


**Figure 15.** Prediction performance of the proposed PSO-based ANN model (testing data).

Similarly, Figures 16 and 17 display the prediction performance of the ICA-based ANN predictive model for the training and testing data, respectively. The R values of 0.967 and 0.994 for the training and testing data, respectively, showed the workability of the ICA-based ANN model for assessing the flexural strength of RRC beams. Despite the relatively good prediction performance of the ICA-based ANN model, the results showed that the PSO-based ANN model outperformed the ICA-based ANN model. To support the aforementioned conclusion, the prediction performances of the ICA-based ANN and PSO-

based ANN models for testing data were assessed using another performance index known as variance accounted for (VAF). VAF can be computed using the following equation:

$$VAF = \left( 1 - \left( \frac{\text{var}(\alpha - \alpha')}{\text{var} \alpha} \right) \right) \times 100 \quad (3)$$

where  $\alpha$  and  $\alpha'$  are measured and predicted values, respectively, and  $\text{var}$  indicates the variance. The model is considered excellent when the VAF value is 100. The obtained VAF values for the recommended PSO-based ANN and ICA-based ANN models were 99.35 and 98.51, respectively. The VAF values also demonstrated the workability of both models. Apart from this, the VAF values showed that the PSO-based ANN model performed better.

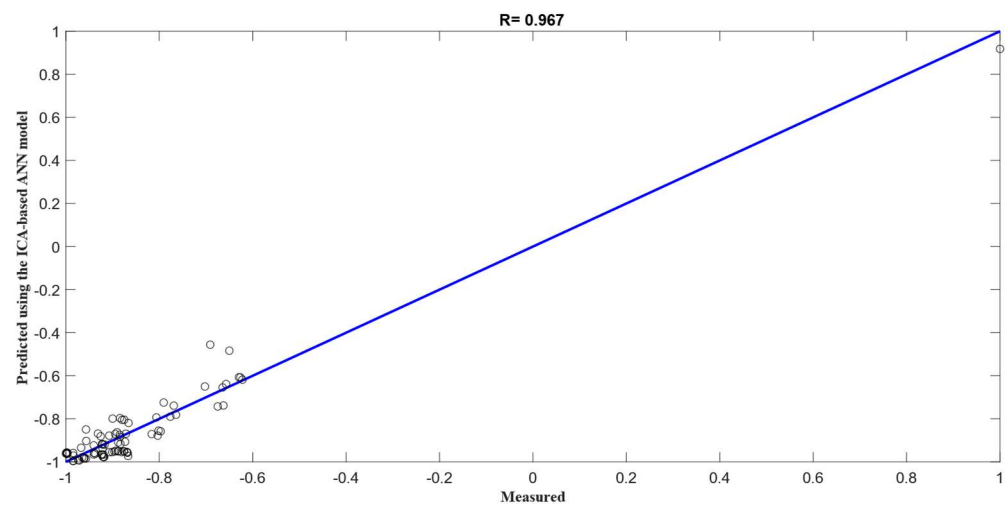


**Figure 16.** Prediction performance of the proposed ICA-based ANN model (training data).

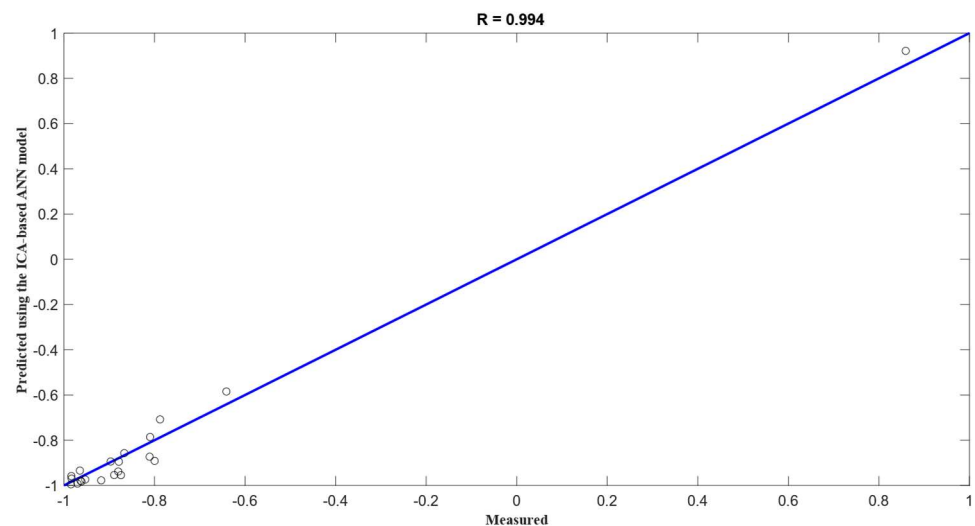


**Figure 17.** Prediction performance of the proposed ICA-based ANN model (testing data).

Figure 18 displays the predicted and measured values of the ultimate flexural strength for the suggested models in this study (i.e., PSO-based ANN model and ICA-based ANN model). As this figure suggests, the predicted values were in good agreement with the measured values. However, the figure shows that the PSO-based ANN predictive model outperformed the ICA-based ANN predictive model.

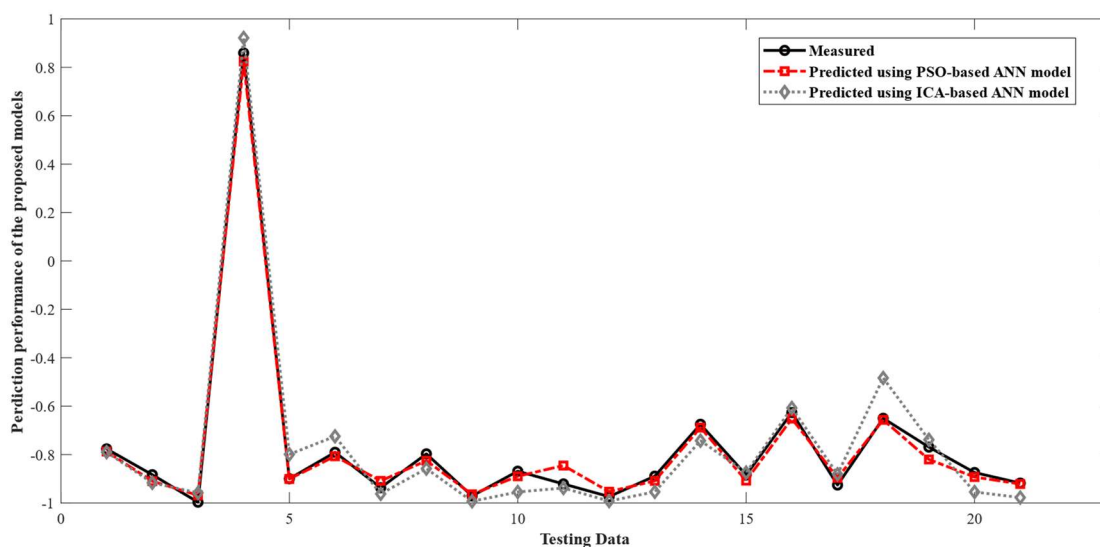


**Figure 18.** Predicted values using the recommended predictive models versus the measured values (testing data).

At last, for comparison purposes, the prediction performance of the PSO-based ANN predictive model was checked against a conventional ANN model (famous backpropagation neural network) with the same structure (i.e., nine hidden nodes). The obtained results for the conventional ANN (i.e., R-value of 0.884 for testing data) showed that the PSO-based ANN model also outperformed the conventional ANN-based predictive model in assessing the flexural behavior of the RRC beams.

## 6. Summary and Conclusions

In this study, two flexural tests were performed on concrete beams. The length, width, and depth of reinforced concrete beams were 1500 mm, 200 mm, and 300 mm, respectively. The results of the flexural tests showed an almost 10% reduction in ultimate flexural strength when recycled aggregates were used instead of natural aggregates. However, using the experimental results of this study, as well as the compiled experimental data from the literature, a relatively comprehensive database with 107 sets of data was created for the soft computing part of the study. The soft computing part of the study comprised the implementation of ANNs that were improved with PSO, as well as ICA for the flexural assessment of RRC beams. Additionally, for comparison purposes, the PSO-based ANN model was compared with the ICA-based ANN model and a conventional ANN, and it was concluded that the PSO-based ANN model worked better compared with the aforementioned models.

It is worth mentioning that the inputs of the predictive models were RCA%, B, d, a/d, L/d,  $\rho$ ,  $f_c$ , and  $F_y$ . Overall, the R-value of 0.997, VAF value of 99.35, and MSE value of 0.08% for the testing data showed that the PSO-based ANN predictive model with nine hidden nodes in one hidden layer was a feasible tool for predicting the ultimate flexural strength of the RRC beams. Despite the promising results, a word of caution is required regarding generalizing the prediction performance of every predictive model. In fact, the reliability of soft computing-based predictive models depends on the quality, quantity, and range of the training data. Hence, when the range of future data is beyond the range of the implemented dataset, the predictability of intelligent models is open to question. In this regard, further research on enhancing the implemented dataset in this study is recommended.

**Author Contributions:** Conceptualization, E.M.; data curation, F.O. and A.E.; formal analysis, E.M.; investigation, E.M., F.O., and A.E.; methodology, E.M.; project administration, F.O. and E.M.; supervision, F.O.; writing—original draft, E.M., A.D., and V.G.; writing—review and editing, E.M., A.D., and V.G. All authors have read and agreed to the published version of the manuscript.

**Funding:** This research received no external funding.

**Institutional Review Board Statement:** Not applicable.

**Informed Consent Statement:** Not applicable.

**Data Availability Statement:** Not applicable.

**Conflicts of Interest:** The authors declare no conflict of interest.

## References

1. Ignjatović, I.S.; Marinković, S.B.; Mišković, Z.M.; Savić, A.R. Flexural behavior of reinforced recycled aggregate concrete beams under short-term loading. *Mater. Struct.* **2013**, *46*, 1045–1059. [\[CrossRef\]](#)
2. Hossain, U.; Sun, C.; Lo, I.M.C.; Cheng, J.C.P. Comparative environmental evaluation of aggregate production from recycled waste materials and virgin sources by LCA. *Resour. Conserv. Recycl.* **2016**, *109*, 67–77. [\[CrossRef\]](#)
3. Soutsos, M.N.; Tang, K.; Millard, S.G. Use of recycled demolition aggregate in precast products, phase II: Concrete paving blocks. *Constr. Build. Mater.* **2011**, *25*, 3131–3143. [\[CrossRef\]](#)
4. Silva, R.V.; de Brito, J.; Dhir, R.K. Properties and composition of recycled aggregates from construction and demolition waste suitable for concrete production. *Constr. Build. Mater.* **2014**, *65*, 201–217. [\[CrossRef\]](#)
5. Sato, R.; Maruyama, I.; Sogabe, T.; Sogo, M. Flexural behavior of reinforced recycled concrete beams. *J. Adv. Concr. Technol.* **2007**, *5*, 43–61. [\[CrossRef\]](#)
6. Kang, T.H.K.; Kim, W.; Kwak, Y.K.; Hong, S.G. Flexural Testing of Reinforced Concrete Beams with Recycled Concrete Aggregates. *ACI Struct. J.* **2014**, *111*, 607–616. [\[CrossRef\]](#)
7. Yehia, S.; Helal, K.; Abusharkh, A.; Zaher, A.; Istaitiyeh, H. Strength and Durability Evaluation of Recycled Aggregate Concrete. *Int. J. Concr. Struct. Mater.* **2015**, *9*, 219–239. [\[CrossRef\]](#)
8. Katerusha, D. Investigation of the optimal price for recycled aggregate concrete—An experimental approach. *J. Clean. Prod.* **2022**, *365*, 132857. [\[CrossRef\]](#)
9. Knaack, A.M.; Kurama, Y.C. Behavior of reinforced concrete beams with recycled concrete coarse aggregates. *J. Struct. Eng.* **2015**, *141*, B4014009. [\[CrossRef\]](#)
10. Arezoumandi, M.; Smith, A.; Volz, J.S.; Khayat, K.H. An experimental study on flexural strength of reinforced concrete beams with 100% recycled concrete aggregate. *Eng. Struct.* **2015**, *88*, 154–162. [\[CrossRef\]](#)
11. Choi, W.C.; Yun, H.D.; Kim, S.W. Flexural performance of reinforced recycled aggregate concrete beams. *Mag. Concr. Res.* **2012**, *64*, 837–848. [\[CrossRef\]](#)
12. Khatib, J. Properties of concrete incorporating fine recycled aggregate. *Cem. Concr. Res.* **2005**, *35*, 763–769. [\[CrossRef\]](#)
13. Sera-Paz, S.; González-Fontebo, B.; Martínez-Abella, F.; Eiras-López, J. Flexural performance of reinforced concrete beams made with recycled concrete coarse aggregate. *Eng. Struct.* **2018**, *156*, 32–45. [\[CrossRef\]](#)
14. Ajdukiewicz, A.B.; Kliszczewicz, A.T. Comparative tests of beams and columns made of recycled aggregate concrete and natural aggregate concrete. *J. Adv. Concr. Technol.* **2007**, *5*, 259–273. [\[CrossRef\]](#)
15. Bai, W.H.; Sun, B.X. Experimental study on flexural behavior of recycled coarse aggregate concrete beam. *Appl. Mech. Mater.* **2010**, *29*, 543–548. [\[CrossRef\]](#)
16. Al-Zahraa, F.I.; El-Mihilmy, M.T.; Bahaa, T.M. Flexural strength of concrete beams with recycled concrete aggregates. *J. Eng. Appl. Sci.* **2010**, *57*, 355–375.
17. Duan, J.; Asteris, P.G.; Nguyen, H.; Bui, X.N.; Moayed, H. A novel artificial intelligence technique to predict compressive strength of recycled aggregate concrete using ICA-XGBoost model. *Eng. Comput.* **2021**, *37*, 3329–3346. [\[CrossRef\]](#)
18. Li, N.; Asteris, P.G.; Tran, T.T.; Pradhan, B.; Nguyen, H. Modelling the deflection of reinforced concrete beams using the improved artificial neural network by imperialist competitive optimization. *Steel Compos. Struct.* **2022**, *42*, 733–745.
19. Mahmood, W.; Mohammed, A.S.; Asteris, P.G.; Kurda, R.; Armaghani, D.J. Modeling flexural and compressive strengths behaviour of cement-grouted sands modified with water reducer polymer. *Appl. Sci.* **2022**, *12*, 1016. [\[CrossRef\]](#)
20. Parsajoo, M.; Armaghani, D.J.; Asteris, P.G. A precise neuro-fuzzy model enhanced by artificial bee colony techniques for assessment of rock brittleness index. *Neural Comput. Appl.* **2022**, *34*, 3263–3281. [\[CrossRef\]](#)
21. Asteris, P.G.; Nguyen, T.A. Prediction of shear strength of corrosion reinforced concrete beams using Artificial Neural Network. *J. Sci. Transp. Technol.* **2022**, *2*, 1–12.
22. Barkhordari, M.S.; Armaghani, D.J.; Asteris, P.G. Structural Damage Identification Using Ensemble Deep Convolutional Neural Network Models. *Comput. Modeling Eng. Sci.* **2022**, *134*, 835–855. [\[CrossRef\]](#)
23. Bardhan, A.; Biswas, R.; Kardani, N.; Iqbal, M.; Samui, P.; Singh, M.P.; Asteris, P.G. A novel integrated approach of augmented grey wolf optimizer and ann for estimating axial load carrying-capacity of concrete-filled steel tube columns. *Constr. Build. Mater.* **2022**, *337*, 127454. [\[CrossRef\]](#)
24. Armaghani, D.J.; Harandizadeh, H.; Momeni, E.; Maizir, H.; Zhou, J. An optimized system of GMDH-ANFIS predictive model by ICA for estimating pile bearing capacity. *Artif. Intell. Rev.* **2022**, *55*, 2313–2350. [\[CrossRef\]](#)
25. Armaghani, D.J.; Asteris, P.G. A comparative study of ANN and ANFIS models for the prediction of cement-based mortar materials compressive strength. *Neural Comput. Appl.* **2021**, *33*, 4501–4532. [\[CrossRef\]](#)

26. Momeni, E.; Yarivand, A.; Dowlatshahi, M.B.; Armaghani, D.J. An efficient optimal neural network based on gravitational search algorithm in predicting the deformation of geogrid-reinforced soil structures. *Transp. Geotech.* **2021**, *26*, 100446. [[CrossRef](#)]
27. Asteris, P.G.; Skentou, A.D.; Bardhan, A.; Samui, P.; Lourenço, P.B. Soft computing techniques for the prediction of concrete compressive strength using Non-Destructive tests. *Constr. Build. Mater.* **2021**, *303*, 124450. [[CrossRef](#)]
28. Le, T.T.; Asteris, P.G.; Lemonis, M.E. Prediction of axial load capacity of rectangular concrete-filled steel tube columns using machine learning techniques. *Eng. Comput.* **2021**, 1–34. [[CrossRef](#)]
29. Naderpour, H.; Mirrashid, M. Shear strength prediction of RC beams using adaptive neuro-fuzzy inference system. *Sci. Iran.* **2020**, *27*, 657–670. [[CrossRef](#)]
30. Lu, S.; Koopialipour, M.; Asteris, P.G.; Bahri, M.; Armaghani, D.J. A Novel Feature Selection Approach Based on Tree Models for Evaluating the Punching Shear Capacity of Steel Fiber-Reinforced Concrete Flat Slabs. *Materials* **2020**, *13*, 3902. [[CrossRef](#)]
31. Asteris, P.G.; Argyropoulos, I.; Cavaleri, L.; Rodrigues, H.; Varum, H.; Thomas, J.; Lourenço, P.B. Masonry Compressive Strength Prediction using Artificial Neural Networks. In Proceedings of the International Conference on Transdisciplinary Multispectral Modeling and Cooperation for the Preservation of Cultural Heritage, Athens, Greece, 10–13 October 2018; Springer: Cham, Switzerland, 2018; pp. 200–224.
32. Kamanli, M.; Kaltakci, M.Y.; Bahadir, F.; Balik, F.S.; Korkmaz, H.H.; Donduren, M.S.; Cogurcu, M.T. Predicting The Flexural Behaviour of Concrete and Lightweight Concrete Beams by ANN. *Indian J. Eng. Mater. Sci.* **2012**, *19*, 87–94.
33. Perera, R.; Barchin, M.; Arteaga, A.; De Diego, A. Prediction of the ultimate strength of reinforced concrete beams FRP-strengthened in shear using neural networks. *Compos. Part B Eng.* **2010**, *41*, 287–298. [[CrossRef](#)]
34. Kaczmarek, M.; Szymańska, A. Application of artificial neural networks to predict the deflections of reinforced concrete beams. *Studia Geotech. Et Mech.* **2016**, *38*, 37–46. [[CrossRef](#)]
35. Bai, C.; Nguyen, H.; Asteris, P.G.; Nguyen-Thoi, T.; Zhou, J. A refreshing view of soft computing models for predicting the deflection of reinforced concrete beams. *Appl. Soft Comput.* **2020**, *97*, 106831. [[CrossRef](#)]
36. Suguna, K.; Raghunath, P.N.; Karthick, J.; Uma Maheswari, R. ANN based modeling for high strength concrete beams with surface mounted FRP laminates. *Int. J. Optim. Civil Eng.* **2018**, *8*, 453–467.
37. Metwally, I. Intelligent predicting system for modelling of reinforced concrete of flexurally strengthened beams with CFRP laminates. *Build Res. J.* **2014**, *61*, 25–42. [[CrossRef](#)]
38. Shanmugavelu, V.A.; Ramachandran, N.; Raghunath, P.N.; Suguna, K. Experimental and analytical studies on reinforced concrete beams with GFRP laminates. *Int. J. Appl. Eng. Res.* **2016**, *1*, 1950–1953.
39. Saadoon, A.S.; Malik, H.S. Prediction of ultimate load of concrete beams reinforced with FRP bars using artificial neural networks. *Al-Qadisiyah J. Eng. Sci.* **2017**, *10*, 11–25.
40. Al-Jurmma, M. Predicting the Ultimate Load Capacity of RC Beams by ANN. *TIKRIT J. Eng. Sci.* **2011**, *18*, 56–66. [[CrossRef](#)]
41. Erdem, H. Prediction of the moment capacity of reinforced concrete slabs in fire using artificial neural networks. *Adv. Eng. Softw.* **2010**, *41*, 270–276. [[CrossRef](#)]
42. Cai, B.; Pan, G.L.; Fu, F. Prediction of the post-fire flexural capacity of RC beam using GA-BPNN Machine Learning. *J. Perform. Constr. Facil.* **2020**, *34*, 04020105. [[CrossRef](#)]
43. Dreyfus, G. *Neural Networks: Methodology and Application*; Springer: Berlin/Heidelberg, Germany, 2005.
44. Kennedy, J.; Eberhart, R. Particle swarm optimization. In Proceedings of the IEEE International Conference on Neural Networks, Perth, Australia, 27 November–1 December 1995; pp. 1942–1948.
45. Atashpaz-Gargari, E.; Lucas, C. Imperialist competitive algorithm: An algorithm for optimization inspired by imperialistic competition. In Proceedings of the IEEE Congress on Evolutionary Computation, Singapore, 25–28 September 2007; pp. 4661–4667.
46. Armaghani, D.J.; Tonnizam Mohamad, E.; Momeni, E.; Monjezi, M.; Sundaram Narayanasamy, M. Prediction of the strength and elasticity modulus of granite through an expert artificial neural network. *Arab. J. Geosci.* **2016**, *9*, 48. [[CrossRef](#)]
47. Momeni, E.; Armaghani, D.J.; Hajihassani, M.; Amin, M.F.M. Prediction of uniaxial compressive strength of rock samples using hybrid particle swarm optimization-based artificial neural networks. *Measurement* **2015**, *60*, 50–63. [[CrossRef](#)]
48. Mahamad, E.T.; Armaghani, D.J.; Momeni, E.; Yazdavar, A.H.; Ebrahimi, M. Rock strength estimation: A PSO-based BP approach. *Neural Comput. Appl.* **2018**, *30*, 1635–1646. [[CrossRef](#)]
49. Rezaei, H.; Nazir, R.; Momeni, E. Bearing capacity of thin-walled shallow foundations: An experimental and artificial intelligence-based study. *J. Zhejiang Univ. A* **2016**, *17*, 273–285. [[CrossRef](#)]
50. Evangelista, L.; De Brito, J. Flexural behaviour of reinforced concrete beams made with fine recycled concrete aggregates. *KSCE J. Civ. Eng.* **2017**, *21*, 353–363. [[CrossRef](#)]
51. Armaghani, J.; Harandizadeh, H.D.; Momeni, E. Load carrying capacity assessment of thin-walled foundations: An ANFIS-PNN model optimized by genetic algorithm. *Eng. Comput.* **2021**, 1–23. [[CrossRef](#)]
52. *ASTM C150*; Standard Specification for Portland Cement. ASTM International: West Conshohocken, PA, USA, 2012.
53. *ASTM D8038-16*; Standard Practice for Reclamation of Recycled Aggregate Base (RAB) Material. ASTM International: West Conshohocken, PA, USA, 2016.
54. *ACI 555*; Building Code Requirements for Structural Concrete and Commentary (ACI 555R-01), ACI Committee 555. American Concrete Institute: Farmington Hills, MI, USA, 2001.
55. *ASTM C125-16*; Standard Terminology Relating to Concrete and Concrete Aggregates. ASTM International: West Conshohocken, PA, USA, 2016.

- 
56. *ASTM D5821-13*; Standard Test Method for Determining the Percentage of Fractured Particles in Coarse Aggregate. ASTM International: West Conshohocken, PA, USA, 2017.
  57. *ASTM C370*; Standard Test Method for Moisture Expansion of Fired Whiteware Products. ASTM International: West Conshohocken, PA, USA, 2016.